Removal of uranium(VI) from aqueous solutions and nuclear industry effluents using humic acid-immobilized zirconium-pillared clay

T.S. Anirudhan*, C.D. Bringle, S. Rijith

Department of Chemistry, University of Kerala, Kariavattom, Trivandrum-695 581, India
Tel. +91 (471) 2418782; Fax +91 (471) 2307158; email: tsani@rediffmail.com

ABSTRACT

Removal of uranium [U(VI)] from aqueous solutions with humic acid-immobilized zirconium-pillared clay (HA-Zr-PILC) was investigated using batch adsorption technique. Maximum removal of 99.2% was observed for an initial concentration of 25 mg L^{-1} at pH 6.0 and an adsorbent dose of 2 g L^{-1}. Equilibrium was achieved in approximately 4 h. The adsorbent was characterized using, XRD, FTIR, SEM, TG/DTG surface area analyzer and potentiometric titration. The effects of pH, contact time, initial concentration and adsorbent dose on removal process were evaluated. The experimental kinetic and isotherm data were analyzed using a second-order kinetic equation and Langmuir isotherm model, respectively. The monolayer adsorption capacity for U(VI) removal was found to be 134.65±4.07 mg g^{-1}. Adsorption experiments were also conducted using a commercial cation exchanger, with carboxylate functionality for comparison. Adsorption efficiency was tested using a simulated nuclear industry effluent sample. Experimental results obtained from repeated adsorption/desorption cycles indicate that the adsorbent can be potentially applied for the removal and recovery of U(VI) ions from various aqueous solutions.

Keywords: Pillared clay; Humic acid; Uranium; Adsorption kinetics; Isotherm; Regeneration

1. Introduction

Uranium is the most important element for nuclear industry. Nuclear power is derived from uranium. Because of the expected shortage of uranium in the near future, efforts have already been made to the recovery of uranium from seawater industry effluents and industrial phosphoric acid. Moreover, the discharge of uranium from nuclear industries and thereby contaminations of surface and groundwater have brought global concern to environmental authorities. The carcinogenic impacts of uranium are well documented and uptake of uranium by human beings can cause health problems such as severe liver damage, kidney damage and eventually death. The drinking water guideline recommended by the US Environmental Protection Agency (EPA) is 0.03 mg L^{-1} [1]. The permissible discharge levels for nuclear industries range from 0.1 to 0.5 mg L^{-1}. Thus, uranium in industry wastewater has to be removed before it is discharged into a water body.

Several techniques are available for the removal of U(VI) ions from aqueous solutions: including chemical precipitation, solvent extraction, micellar ultrafiltration, ion exchange and adsorption. Among these adsorption technique is considered to be very important because of its cost effective treatment, easy operation, narrow space

_____

* Corresponding author.

for building the plant, no chemical reagents needed and no sludge produced.

A number of adsorbent materials are being investigated for the removal of U(VI) ions from aqueous solutions. They include interpenetrating polymer network, modified chitosan resins, cross linked poly 2,2-bisacrylamido acetic acid, phytic acid modified polyacrylamide-bentonite composite, chemically modified polyurethane foam and polymer grafted lignocelluloses [2–7]. Natural clays are also being considered as alternative low-cost adsorbents for this purpose [8]. Various types of clays as low cost adsorbents for heavy metal removal have been reported [9]. Bentonite is well defined naturally occurring 2:1 aluminosilicate mineral consists of one alumina octahedral layer sandwiched between two silica tetrahedral layers. The potential adsorption sites for metal ions on bentonite include silanol, $\equiv SiOH$ and aluminol, $\equiv AlOH$, hydroxyl groups on the mineral edges and the permanently charged sites, $\equiv X^-$, on the basal surfaces. The adsorption properties of bentonite can be improved by surface modification. The pillaring of certain metal oxides into bentonite results in increase in basal spacing, surface area and pore and produces a structure with two dimensional micropores. The application of pillared clays (PILCs) for environmental pollution control in terms of metal removal from aqueous media has received much attention [10,11]. It was also reported that the adsorption capacity of Al_{13}-pillared bentonite for Co(II) ions is as high as that of non-pillared bentonite [12]. The values of surface area, porosity and cation exchange capacity were found to be higher for Al_{13}-PILC compared to that of Na-bentonite. The decrease in pH of zero point charge after pillaring indicates that the surface become more negative and this helps to adsorb positively charged Co(II) species through electrostatic interaction. The ability of Zr, Al and lanthana alumina mixed oxide pillared clays to remove humic acid (HA) from aqueous solutions was also investigated by earlier workers [13–15]. The regeneration of spent adsorbent is an equally important aspect of the process. In many cases after two or three cycles of repeated use the adsorbent material cannot be reused causing a disposal problem. One of the possible approaches for the disposal of the spent adsorbent, HA loaded-PILC (HA–PILC) is its use again as an adsorbent for treating wastewater containing other pollutants. It is widely recognized that HAs have an elevated cation exchange capacity and form complex with heavy metals because they contain carboxylic and phenolic hydroxyl groups in their structure. The objective of this work is to determine the feasibility of using HA-loaded Zr–PILC as an adsorbent for the removal of U(VI) ions from water and nuclear industry wastewater. It was proposed to take advantage of the cation exchange capacity of the HA from the adsorbent surface to remove U(VI) ions from aqueous solutions.

2. Experimental

2.1. Materials

Analytical grade chemicals were used through out the investigation. The stock solution of U(VI) was prepared by dissolving an accurately weighed amount of uranyl nitrate hexahydrate salt, $UO_2(NO_3)_2.6H_2O$ (Fluka), in distilled water so as to yield a metal ion concentration of 1000 mg L^{-1}. The solution was used as standard solution in the analysis of uranium in liquid phase. Appropriate aliquots were taken from the standard for subsequent dilution to the desired concentration levels. Bentonite sample used in this study was obtained from M/s. Ashapura Clay Mines, Gujarat. Chemical composition of bentonite sample was determined by the usual analytical methods for silicate minerals. Standard chemical analysis along with instrumental methods was used [16]. Al_2O_3, CaO and MgO were analysed with titrimetric method and SiO_2 was analysed with gravimetric method. Fe_2O_3, TiO_2, Na_2O and K_2O were determined by atomic absorption spectroscopic (AAS) method. The chemical composition of bentonite is: 53.1% SiO_2, 13.9% Al_2O_3, 11.5% Fe_2O_3, 0.96% TiO_2, 2.9% CaO, 5.4% MgO, 3.2% Na_2O, 0.55% K_2O and 5.8 % loss on ignition. Zirconium oxychloride ($ZrOCl_2.8H_2O$) (Fluka, Switzerland) was used for pillaring. The stock solution of HA (1675 mg L^{-1}) prepared in distilled water using humic acid (Fluka, Switzerland).

2.2. Adsorbent preparation

The Na-bentonite (Na-B) was prepared by stirring the raw bentonite sample with 1.0 M NaCl using a flask shaker for 24 h. This was followed by washing several times with distilled water. Zirconium-pillared (Zr-PILC) clay was prepared according to the method described by Dyer et al. [17]. Schematic representation of the pillaring process is given in Fig. 1. Exactly 500 mL aqueous solution of 0.1 M zirconium oxychloride ($ZrOCl2.8H2O$) was refluxed at 40°C for 2 h and added dropwise to a Na-B suspension (10 g L^{-1} distilled water) with vigorous stirring. The resulting suspension was aged for 4 h at 90°C. After ageing, the Zr-PILC was separated by centrifugation and washed with deionised water until the supernatant was free from chloride, as indicated by the absence of any white precipitate with silver nitrate solution. The product was then dried, ground and heated at 150°C for 3 h. The Zr-PILC particles were sieved to obtain –80+230 mesh size. This powdered sample was then used for the preparation of humic acid immobilized-Zr-PILC (HA-Zr-PILC). HA was impregnated on Zr-PILC at pH 3.5 using the batch adsorption techniques. A total of 0.1 g Zr-PILC was added to 50 mL aqueous solution of HA of varying concentration ranging from 40 to 500 mg L^{-1}. The initial pH of the solution (pH 3.5) was adjusted and the flasks were shaken at 200 rpm for 24 h. Preliminary studies showed that 24 h duration was sufficient for achieving
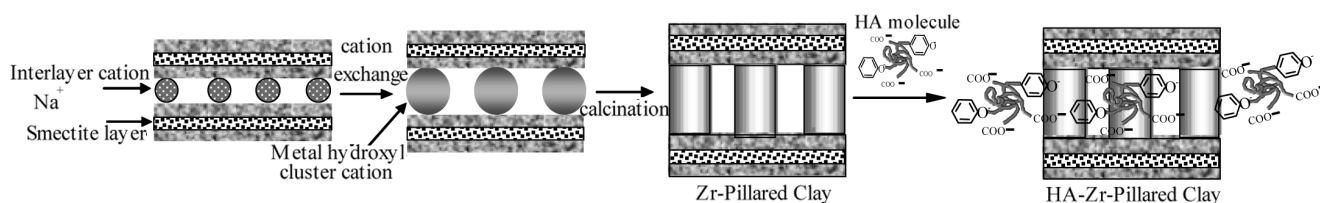
Fig. 1. Preparation of humic acid-immobilized zirconium-pillared clay (HA-Zr-PILC).

equilibrium conditions. After attaining equilibrium, the suspension was centrifuged and the residue was washed with 0.01 M NaClO$_4$ followed by deionised water. The HA-Zr-PILC was dried at 60°C for 24 h. The HA amounts adsorbed were determined from the initial and final concentration of the HA solutions. The concentration of HA in supernatant was analyzed using UV-Visible spectrophotometer at 400 nm. The sorption isotherm was obtained by plotting the amount of HA adsorbed (q_e) vs. equilibrium concentration (C_e). The maximum amount of HA loaded in the Zr-PILC was calculated and found to be 85.50 mg g^{-1}.

2.3. Equipment and methods of characterization

FTIR spectroscopy was used to detect frequency changes in the original and modified bentonite samples. The spectra were collected by a Perkin-Elmer FTIR-180 spectrophotometer within the wavelength range 400–4000 cm^{-1} using a KBr window. The pellets were prepared by mixing 1 mg sample with 100 mg IR grade KBr. A scanning electron microscope (Philips model XL-30CP) operated at 12 kV was used to study surface morphology changes of the adsorbent. The X-ray diffraction patterns of the adsorbent samples were recorded in a Rigaku Dmax (IC model) X-ray diffractometer using Cu K$_\alpha$ radiation. The surface area of the adsorbent was determined by using methylene blue adsorption method [18]. The point of zero charge (pH$_{pzc}$) of the adsorbents was determined using potentiometric method [19]. The density of the adsorbents was estimated using specific gravity bottle [20]. A Metler Toledo thermal analyzer was used to study the thermal stability of the adsorbent samples. The pH measurements were made using a Systronic microprocessor pH meter (Model μ 362, India). The concentration of U(VI) ions in the supernatant solutions was measured using UV-visible spectrophotometer (Jasco V-530). A temperature controlled water bath shaker (Remi, model-G-16, India) with a temperature variation of ±1.0°C was used for equilibrium studies.

2.4. Adsorption experiments

Batch adsorption experiments were performed using 0.1 g of adsorbent with 50 mL of aqueous metal ion solutions in 100 mL Erlenmeyer flasks of which concentration, pH, and temperature have already been known. The contents were shaken at 200 rpm in a shaking water bath. After required contact time, supernatant was analyzed for U(VI). For the sorption kinetic studies, initial concentration of U(VI) was kept in the range 100–250 mg L^{-1}. Effect of pH of the medium on U(VI) removal was studied in the pH range 2.0–7.0 using two different initial concentrations of 25 and 50 μmol L^{-1}. Initial solution pH was adjusted to required pH levels using either 0.01 M HNO$_3$ or 0.01 M NaOH. Isotherm studies were conducted with 2 g L^{-1} adsorbent dose and varying initial concentration of U(VI) (25–400 mg L^{-1}). The concentration of U(VI) in the supernatant was measured using spectroscopic method [21] based on coloured complex with sodium diethyldithiocarbamate in aqueous medium. The yellow coloured complex in solution was measured using a UV- visible spectrophotometer at 460 nm and the calibration of U(VI) concentrations is performed by means of the respective calibration curve. The adsorption capacity was calculated using the following mass balance equation:

$$q_e = \frac{(C_0 - C_e)V}{W} \tag{1}$$

where q_e is the equilibrium adsorption capacity (mg g^{-1}), C_o and C_e is the initial and equilibrium liquid-phase solute concentration (mg L^{-1}), respectively, V is the liquid phase volume (L) and W is the amount of adsorbent (g).

Batch adsorption experiments were also conducted to determine the sorption capacity of a commercial synthetic polymer-based cation exchange resin. For this purpose, a commercial carboxylate functionalized cation exchanger Ceralite IRC-50 (similar to Amberlite IRC-50) obtained from the Central Drug House, Mumbai, India was used. To ensure the accuracy, reliability and reproducibility of the collected data, all batch experiments were carried out in duplicate and the mean values of two data sets are presented. In all instances the accuracy of the data was very good, as the relative standard deviation was < 4.0%. When the relative error exceeded this criterion, the data were disregarded and a third experiment was conducted until the relative error fall within an acceptable range.

2.5. Desorption and regeneration studies

The spent adsorbent was thoroughly washed with deionised water. Desorption studies using spent adsorbent were carried out using 50 mL HCl acid having different

concentrations. HA-Zr-PILC loaded with U(VI) ions was placed in the desorption medium and stirred at 200 rpm for 4 h. After agitation, the supernatant solution was analysed for U(VI) ions. The percentage of desorption was calculated from the amount of U(VI) adsorbed on HA-Zr-PILC and the final U(VI) ion concentration in the desorption medium. Adsorption-desorption cycles were repeated four times by using the same adsorbent.

3. Results and discussion

3.1. Humic acid loading on Zr-PILC

To optimize the pH value for HA loading onto Zr-PILC from aqueous solution, experiments were carried out by varying the pH over the range 2.0–7.0 (Fig. 2). It is seen from this figure that the maximum HA adsorption was achieved at pH 3.5 and decrease after pH > 3.5 is due to the external hydrogen bond formed between phenolic hydroxyl groups of HA and the hydrogen bonding sites on the clay. The undissociated HA molecules dominating at low pH are hydrophobic and more absorbable than the ionized form as the hydrogen bond becomes the driving force for adsorption.

The equilibrium adsorption isotherm is essential in determining the adsorption capacity of the Zr-PILC for immobilizing HA and for knowing the nature of adsorption. The equilibrium adsorption isotherm of Zr-PILC was obtained at 30°C by mixing 0.1 g of the adsorbent with 50 mL of HA solution of varying concentration (40–500 mg L^{-1}) at pH 3.5 (Fig. 3). It is observed that the adsorption capacity increases as a function of HA concentration. The maximum adsorption capacity towards HA was found to be 85.50 mg g^{-1}. The protonated or undissociated HA molecules dominating at pH 3.5 are more hydrophobic and more adsorbable than the ionized form as the hydrophobic bonding becomes the driving force for adsorption [22]. The possibility of interlamellar adsorption of HA on clays and PILC's has also been discussed in the literature [13,22,23]. It is also assumed that HA molecules react with Zr-PILC by adsorbing on its surface and also by entering into the interlayer surfaces. After knowing the maximum loading capacity of Zr-PILC, 10.0 g Zr-PILC was loaded with HA at its optimum concentration and pH 3.5 in order to further investigate the adsorption characteristics for U(VI). Preparation of HA immobilized Zr-PILC (HA-Zr-PILC) is given in Fig. 1.

3.2. Adsorbent characterization

3.2.1. SEM, XRD, IR and TG analyses

Scanning electron microscopy (SEM) was used to study the morphological features of Na-B, Zr-PILC and HA-Zr-PILC. The surface morphology of Na-B is different from that of Zr-PILC and HA-Zr-PILC (Fig. 4). The Na-B before pillaring appears as their cornflake like crystal with
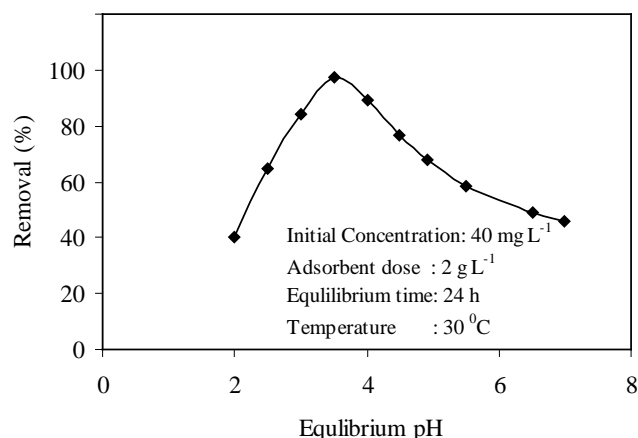

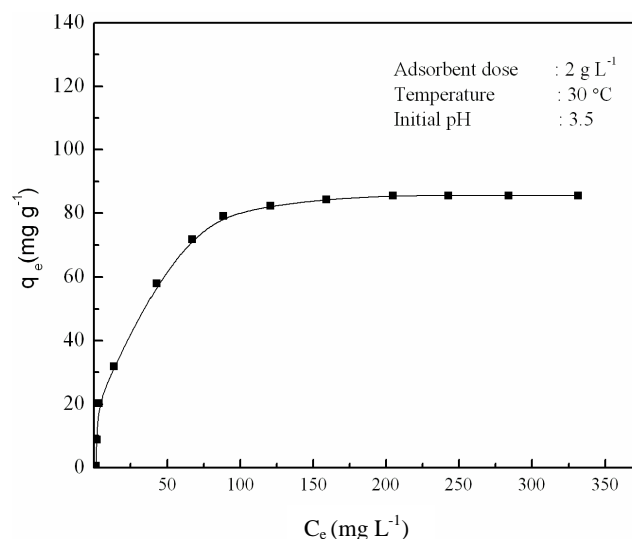Fig. 2. Effect of pH on HA adsorption onto Zr-PILC.

Fig. 3. q_e vs. C_e plots for adsorption of HA onto Zr-PILC.

fluffy appearance revealing the extremely fine platy structure. After pillaring the clay has become more porous and fluffy. This porous and fluffy appearance probably occurs due to the change in surface charge of the particle as a result of pillaring and the reduction in certain amorphous phase originally associated within the Na-B. The surface of Zr-PILC appears rougher than that of Na-B. After HA immobilization onto Zr-PILC, the pores are wide open and well defined which makes it an excellent adsorbent for both organic and inorganic contaminants.

Comparative XRD patterns of Zr-PILC, HA-Zr-PILC and U(VI)-HA-Zr-PILC are shown in Fig. 5. XRD patterns of Zr-PILC showed a d-spacing of 12.5, 7.49 and 1.80 Å at 2θ values of 2.76, 4.6 and 19.2. HA-Zr-PILC has an increased d spacing of 19.5 Å (2θ = 1.8), and another peak at 20.4 (1.7 Å) is also seen. After adsorption of U(VI) onto HA-Zr-PILC the 2θ values are only slightly changed
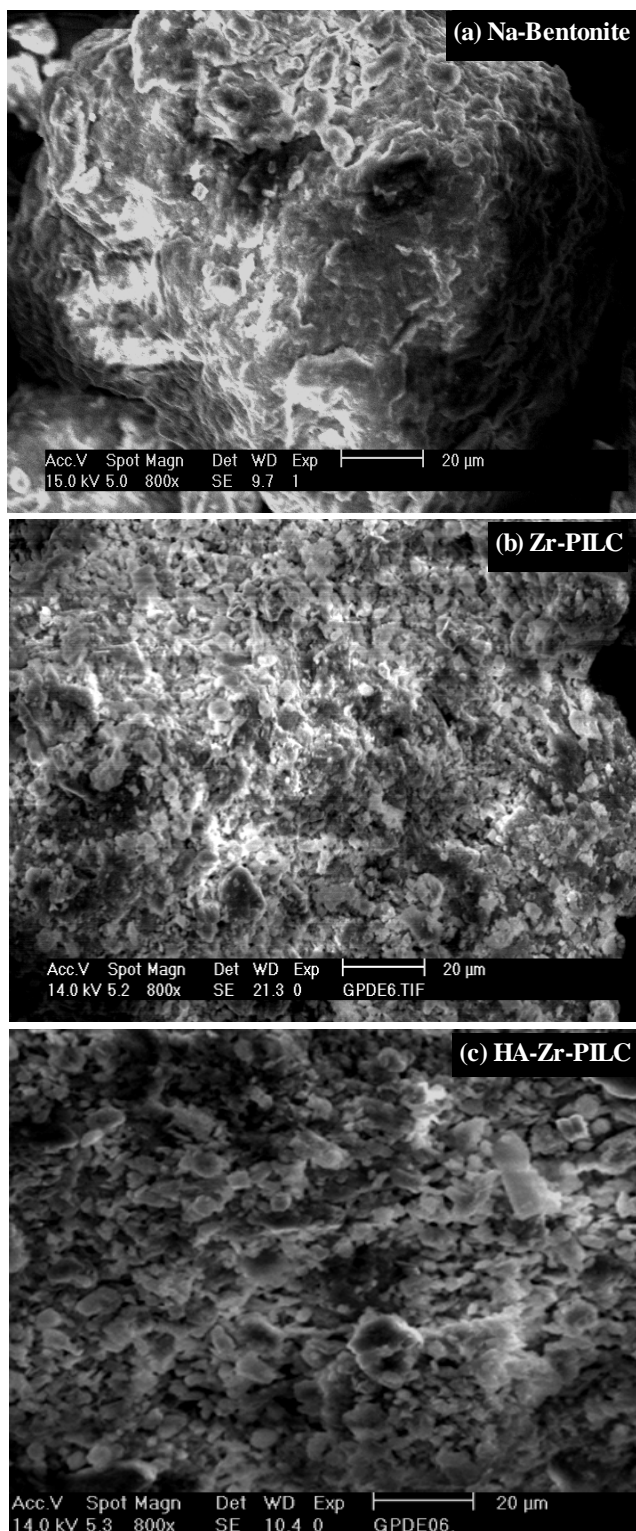
Fig. 4. SEM photographs of (a) Na-B, (b) Zr-PILC and (c) HA-Zr-PILC.

Fig. 5. X-ray diffraction patterns of Zr-PILC, HA-Zr-PILC and U(VI)-HA-Zr-PILC.

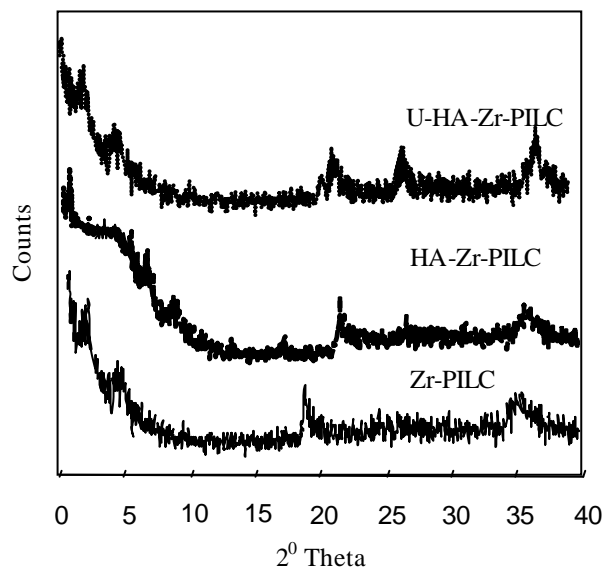and the appearance of new reflections at 20.1 and 27.3 indicates U(VI) adsorption onto HA-Zr-PILC. Intercala-

tion followed by calcination of a material usually results in reduction of crystallinity and the material becomes amorphous to XRD. Calcination leads to a decrease in the basal spacings, which is sometimes accompanied by structural collapse. The intercalated clays are usually better ordered than their parent clays, but this ordering cannot withstand calcination, which is reflected in fewer XRD peaks or no low-angle peaks.

The FTIR spectra of Na-B, Zr-PILC, HA-Zr-PILC and U(VI)-HA-Zr-PILC are shown in Fig. 6. For Na-B, some characteristic peaks are observed at 3641, 3622 and 3604 cm^{-1} which are due to the presence of absorption bands corresponding to Si–O, Al–O and Na–O vibrations for Na-B. The broad peak observed in the region 3300–3500 cm^{-1} is exactly for Na-B corresponding to different stretching vibrations of different hydroxyl groups. The absorption band at 1710 cm^{-1} related to Si–O vibrations. To a certain extent, the spectra of bentonite is very much similar to that amorphous silica showing some absorption bands in the region of 1000–1015 cm^{-1}. Peaks at 516 and 468 cm^{-1} arises due to the stretching and bending vibrations of SiO_4^{2-} tetrahedra [24]. The absorption band at 684 cm^{-1} iis attributed to coupled Al–O and Si–O out of plane vibrations [24]. The peak at 1080 cm^{-1} is due to the silicate ions. The peak at 430 cm^{-1} is due to the O–Si–O bending modes (asymmetric).

In the case of Zr-PILC, the hydrogen bonded –OH stretching and the bending modes of Zr-PILC are seen in the region 3600–3700 cm^{-1}. On calcination, dehydration of interlayer water species occurs to a certain extent. The shifting is also due to the attachment of zirconium to bentonite. The shifting and broadening of some peaks are seen in the region 900–1100 cm^{-1} due to the formation
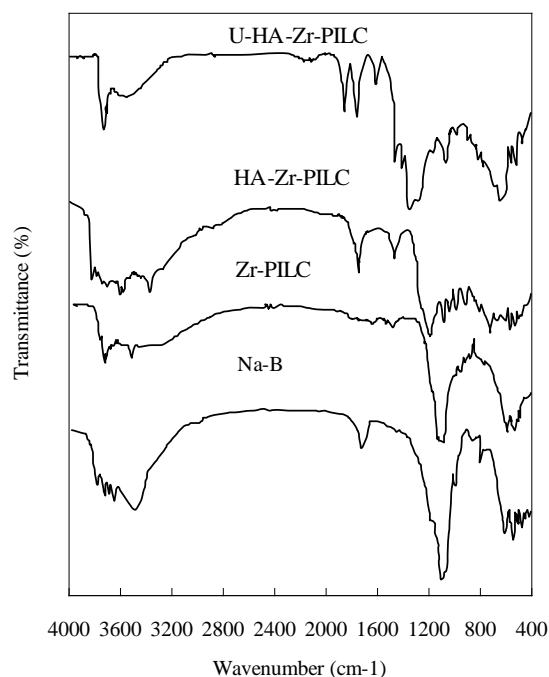
Fig. 6. FTIR spectra of, Na-B, Zr-PILC, HA-Zr-PILC and U(VI)-HA-Zr-PILC.

of protonic sites associated with Si–OH– Zr bridges, appeared due to the calcination process. The intensity reduction may also be due to the sintering of the pillars and the temperature induced decomposition of the intrinsic structure of the bentonite itself.

In HA–Zr–PILC peaks similar to that of bentonite structure is seen in the region 3350–3420 cm⁻¹ which indicates Si–O, N–H and O–H stretching vibrations. The characteristic peak for –COOH group seen at 1720 and 1453 cm⁻¹. Another difference from the parent peak is the appearance of four peaks at 900, 845, 775 and 600 cm⁻¹ which clearly indicates the presence of polyphenyls in humic acid. A medium peak is seen at 918 cm⁻¹ which is –OH out of plane bending of –COOH group which is hydrogen bonded to another carboxylic group.

In the case of U–HA-Zr-PILC, since the hydrogen ions get replaced from the –COOH group, a peak is found at 1380 cm⁻¹. This is due to the conversion of the acid group into its inorganic salt. Also the characteristic –COOH peak at 1720 cm⁻¹ is shifted to 1670 cm⁻¹ region, indicating the replacement of H⁺ ion with metal ions. Also the broad peaks is absent in the region 3300–3400 cm⁻¹ which means the absence of –OH stretching. An absorption band of uranyl (VI) ion is seen at 696 cm⁻¹ which is absent in the spectrum of HA-Zr-PILC.

The TG and DTG curves of the Na-B, Zr-PILC and HA-Zr-PILC are shown in Fig. 7. TG curves exhibit an initial dry weight loss of 9.3% for Na-B between 40°C and 180°C whereas for Zr-PILC an initial weight loss of 12.9% starting at 40°C and ending at 200°C. Below 400°C decom-
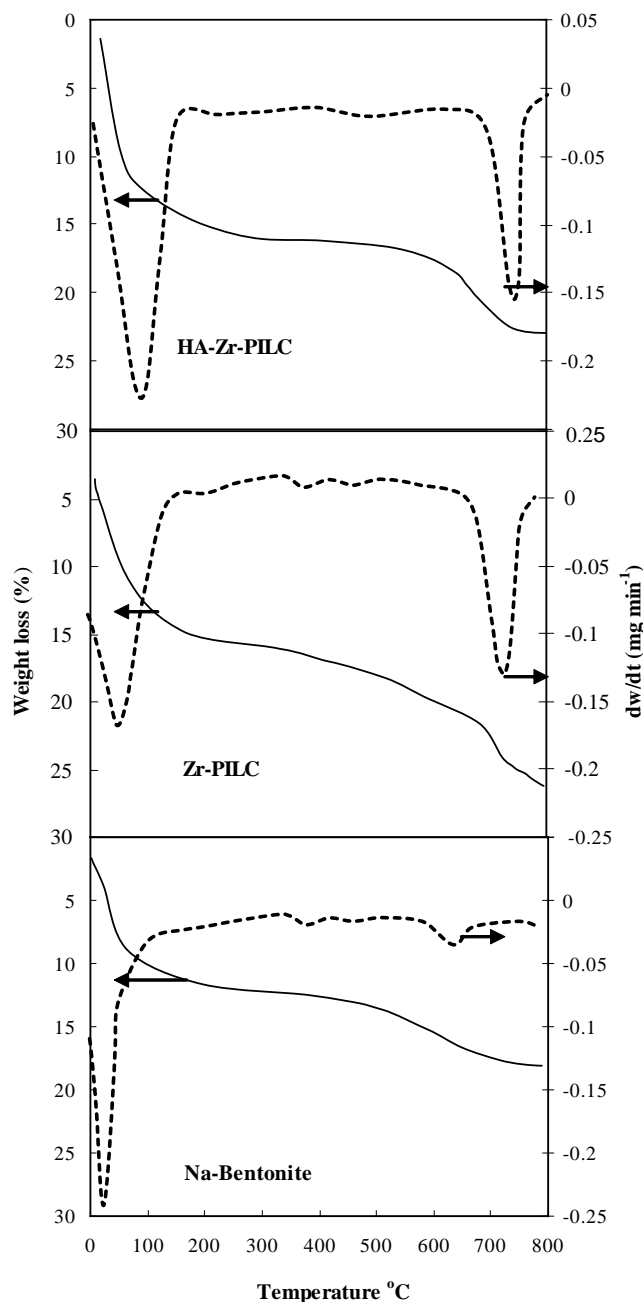

Fig. 7. TG and DTG curves of Na-B, Zr-PILC and HA-Zr-PILC.

position takes place with a weight loss of 10.4 and 15.8% due to the loss of adsorbed water present in Na-B as well as the solvated water in Zr-PILC. Major decomposition takes place above 400°C with a weight loss of 15.1% and 26.1%, respectively for Na-B and Zr-PILC due to the dehydroxylation of the bentonite layer and the intercalated Zr-PILC. The higher weight loss observed in Zr-PILC may be due to the presence of hydrated intercalated species in the interlayer region. In the case of HA-Zr-PILC having two stages of decomposition, first occurs at 110°C with a weight loss of 10.8% due to dehydration. The second

decomposition of HA-Zr-PILC occurs at 670°C, in which a weight loss of 22.4% is produced by dehydroxylation and also by the decomposition of HA. From these results it is clear that HA-Zr-PILC has higher thermal stability. DTG curves show that the decomposition of Na-B, Zr-PILC and HA-Zr-PILC are produced in two steps with maximas, the first ones at 87, 71 and 80°C, second ones at 640, 715 and 738°C, respectively.

Density of the adsorbents was calculated by Pycnometric method in which nitrobenzene was used as a displacing liquid. The density of Na-B, Zr-PILC and HA-Zr-PILC was found to be 1.87, 1.23 and 1.43 g mL^{-1}, respectively. The values of CEC of Na-B, Zr-PILC and HA-Zr-PILC were found to be 0.87, 0.83 and 1.87 meq g^{-1} respectively. The adsorption characteristics of an adsorbent can be obtained from the point zero charge determination. The pH of point of zero charge (pH$_{pzc}$) is defined as the pH at which surface charge density σ_0 is zero. The values of σ_0 was determined by potentiometric titration method using the equation

$$\sigma_0 = F\left[\left(C_A - C_B\right) + \left(OH^- - H^+\right)\right] / A \qquad (2)$$

where F is the Faraday constant, C_A and C_B are the concentrations of strong acid and strong base after each addition during titration. H$^+$ and OH$^-$ ions are the equilibrium concentration of H$^+$ and OH$^-$ ions bound to the suspension surface and A is the surface area of the suspension. About 0.1 g of adsorbent was added to 50 mL of 0.1 M NaNO$_3$. Measured the volumes of alkali and acid required to change the pH. A graph was plotted with σ_o against pH (Fig. 8). The point of intersection of σ_0 with the pH curves give the pH$_{pzc}$. The values of pH$_{pzc}$ were found to be 4.0±0.2, 3.2±0.3 and 2.7±0.2 for Na-B, Zr-PILC and HA-Zr-PILC, respectively. The decrease in pH$_{pzc}$ after HA-loading indicates that the surface of HA-Zr-PILC become more negative and this helps to adsorb positively charged uranyl ion species through electrostatic interaction.
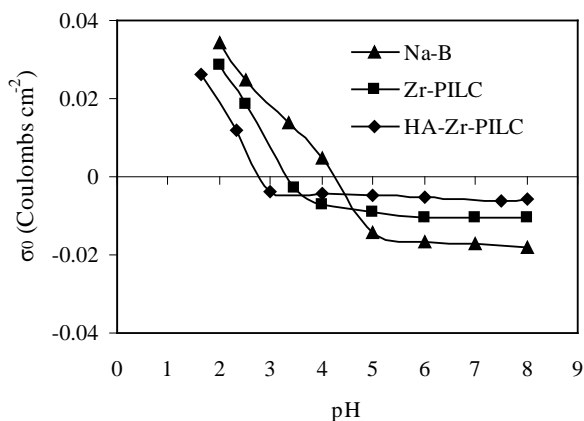
The surface area of the adsorbent was determined using methylene blue (MB) adsorption methods at 30°C. The adsorption of MB on clay samples, as a function of initial concentration at 30°C was studied by the addition of 50 mL of MB solution of varying concentration (1.0×10^{-6}–5.0×10^{-3} M) using 100 mg of the adsorbent. After equilibrium, the supernatant solution was collected and the concentration of MB was determined spectrophotometrically at a wavelength of 660 nm. The values of M_f were obtained from the isotherm graph by extrapolating the "knee point" to the q_e axis and taken as the point of monolayer coverage. The surface area of adsorbent was obtained by substituting the value of M_f in the equation given below:

$$S = M_f \, N_A A_m \cdot 10^{-20} \text{ m}^2\text{g}^{-1} \qquad (3)$$

where M_f is the amount of MB adsorbed per 100 mg of the adsorbent when the surface is completely covered with a monolayer of MB. N_A is the Avogadro number and A_m is the cross-sectional area per molecule of surface. Surface area was found to be 31.9, 42.6 and 49.7 m^2 g^{-1} for Na-B, Zr-PILC and HA-Zr-PILC, respectively. The higher surface area of HA-Zr-PILC is due to the enhanced adsorption of MB in the favorable sites of the poly functional groups, which are present in humic acid.

3.3. Adsorption experiments

3.3.1. Effect of adsorbent dose

Adsorption experiments were conducted to study the effect of adsorbent dose on adsorption of U(VI) onto Zr-PILC and HA-Zr-PILC. Amount of Zr-PILC and HA-Zr-PILC selected for the study ranged between 0.5 and 6 g in 1 L solution. The amount of adsorbed uranium is greater for HA-Zr-PILC, when compared to Zr-PILC as shown in Fig. 9. It is shown that the percentage of adsorption increases with increasing adsorbent doses. For

Fig. 8. Surface charge density of HA-Zr-PILC as a function of pH in aqueous solution of NaNO$_3$.
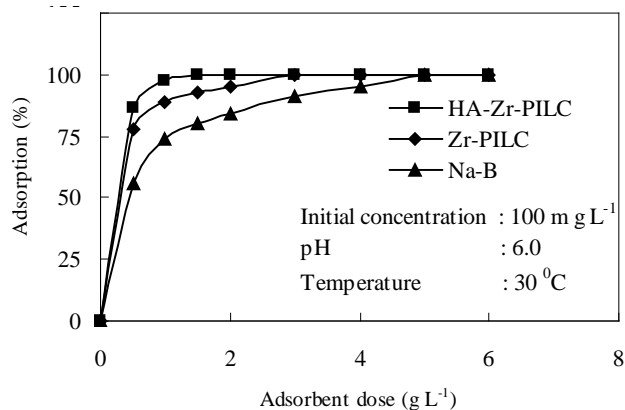

Fig. 9. Effect of adsorbent dose for the adsorption of U(VI) ions onto HA-Zr-PILC.

the complete removal of U(VI) ions from 50 mL aqueous solution containing 100 mg L^{-1} U(VI), a maximum adsorbent dosage adsorbent dosage 2.0 g of HA-Zr_PILC or 3.0 g of Zr-PILC or 5.0 g of Na-B is required These results show that HA-Zr-PILC is more effective than Zr-PILC and Na-B, it is due to the presence of HA with functional groups such as –COOH, Phenolic –OH, –NH and –C=O on HA-Zr-PILC.

3.3.2. Adsorption kinetics

Kinetics has a direct influence on the amount of the adsorbed substance. In the present study, kinetic experiments were performed with four different concentrations of U(VI) solution. The concentrations selected for this study were 100, 150, 200 and 250 mg L^{-1}. The amount of U(VI) adsorbed per unit weight of the adsorbent was determined at definite intervals of time. The adsorption of U(VI) onto HA-Zr-PILC can be described as a function of the contact time as shown in Fig. 10. The results show that as the initial metal concentration increased, the absolute removal of U(VI) ions from solution increased.

The U(VI) adsorption increased with time and attained equilibrium within 150–180 min. A further increase in contact time negligible effect onto U(VI) adsorption. Although equilibrium time was different for different initial concentrations, adsorption in all concentrations completed within 180 min. Therefore, a contact time of 180 min was selected for all subsequent adsorption experiments. The adsorption is higher in the beginning due to greater number of reaction sites available for the adsorp-

tion of U(VI) ions. The amount of U(VI) ions adsorbed per unit mass of the adsorbent increased with the initial metal concentration. With the increase of initial U(VI) concentration from 100 to 250 mg L^{-1}, the adsorption capacity increases from 39.68±1.3 to 101.81±2.71 mg g^{-1}, indicating that U(VI) adsorption depends on the initial metal concentration.

Two kinetic models namely pseudo-first-order and pseudo-second-order models have been used to describe the kinetics of adsorption. The pseudo-first-order [25] kinetic equation may be written as

$$q_t = q_e\left(1 - e^{-k_1 t}\right) \tag{4}$$

whereas the pseudo-second-order equation may be expressed as

$$q_t = \frac{k_2 q_e^2 t}{1 + k_2 q_e t} \tag{5}$$

where q_e and q_t are the amounts of solute adsorbed per unit mass of the adsorbent at equilibrium and time t, respectively. k_1 and k_2 are the pseudo-first-order and pseudo-second-order rate constants, respectively. Parameters of the pseudo-first-order and pseudo-second-order kinetic models were estimated from the experimental data using non-linear curve fitting procedure and the results are presented in Table 1.

To check the variation of both equations visually, the theoretical lines using these constants are also shown in Fig. 10. It also seems that pseudo-second–order equation

Table 1
Kinetic parameters for the adsorption of U(VI)-HA-Zr-PILC

| Kinetic constants	Concentrations (mg L^{-1})			
	100	150	200	250
Pseudo-first-order				
k_{ad} (min^{-1})	3.41±0.09×10^{-1}	2.30±0.12×10^{-1}	2.20±0.04×10^{-1}	2.05±0.07×10^{-1}
R^2	0.994	0.989	0.985	0.988
χ^2	0.512	0.721	0.913	0.765
Pseudo-second-order				
k_2 (g mg^{-1} min^{-1})	3.30±0.15×10^{-2}	2.20±0.05×10^{-2}	1.50±0.02×10^{-2}	1.10±0.03×10^{-2}
q_e (mg g^{-1})	42.50±1.74	61.50±3.00	89.06±3.20	101.50±2.00
R^2	0.999	0.999	0.999	0.999
χ^2	0.145	0.112	0.097	0.054
External diffusion				
B_L (cm s^{-1})	9.68±0.38×10^{-5}	8.03±0.27×10^{-5}	6.12±0.30×10^{-5}	5.10±0.31×10^{-5}
R^2	0.957	0.928	0.898	0.891
χ^2	1.12	0.976	0.876	1.65
Intraparticular diffusion				
D_i (cm^2 s^{-1})	8.54±0.40×10^{-14}	8.15±0.42×10^{-14}	7.56±0.26×10^{-14}	7.10±0.30×10^{-14}
R^2	0.999	0.999	0.999	0.999
χ^2	0.043	0.027	0.091	0.101
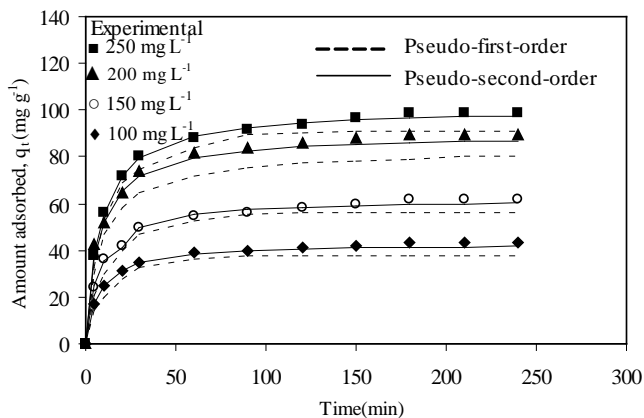
Fig. 10. q_t vs. time plots for the adsorption of U(VI) ions onto HA-Zr-PILC.

fit well with the experimental data. Also the values of R^2 and χ^2 listed in Table 1 reflect a better correlation for the pseudo-second-order model. These results imply that a chemisorption like mechanism may play an important role for the adsorption of U(VI) ions onto HA-Zr-PILC. The adsorption of U(VI) takes place through ion-exchange process until the surface functional groups are freely occupied, thereafter U(VI) ions diffuse into the interlamellar cavities for further interactions. The values of k_2 seem to decrease with increasing metal concentration, which is consistent with studies reported before [26,27].

The rate of attainment of equilibrium may either be explained mass transfer diffusion or intraparticle mass transfer diffusion. The external mass transfer analysis of uranium during the adsorption process by HA-Zr-PILC was studied using the kinetic model developed by McKay et al. [28].

$$\ln\left[\left(\frac{C_t}{C_0}\right) - \frac{1}{(1+mK_L)}\right]$$
$$= \ln\left[\frac{mK_L}{(1+mK_L)}\right] - \left[\frac{(1+mK_L)}{mK_L}\right]B_L S_S \cdot t \quad (6)$$

where C_t is the concentration of adsorbate at time t, C_o is the initial concentration of the adsorbate, m is the mass of the adsorbent per unit volume of particle free adsorbate solution, K_L is the Langmuir constant (Obtained by multiplying Q^o and b). S_s is the specific surface per unit volume of particle free slurry and B_L is the mass transfer coefficient (cm s^{-1}).

The values of B_L were determined from the slope of the plots of ln $[C_t/C_0 - (1 + mK_L]$ vs. t for different concentrations (figure not shown) using regression analysis. The results are presented in Table 1. From the table it is clear that the B_L values decrease from $9.68\pm00.38\times10^{-5}$ to $5.10\pm0.31\times10^{-5}$ cm s^{-1}, when the initial concentration increases from 100 to 250 mg L^{-1}, since increasing the

metal concentration in the solution reduced the diffusion of metal ions in the boundary layers.

Besides the adsorption at the surface of the adsorbent, the adsorbate molecule may also diffuse into the interior of the porous adsorbent. The diffusion constant for the adsorption of uranium by HA-Zr-PILC was calculated using the following equation developed by Urano and Tachikawa [29].

$$f\left[\frac{q_t}{q_e}\right] = -\log\left[\left(\frac{q_t}{q_e}\right)^2\right] = \frac{4\pi^2 D_i t}{2.303 d^2} \quad (7)$$

where q_t and q_e are the amounts of U(VI) adsorbed at time t and at equilibrium, respectively, d is the diameter of the adsorbent and D_i is the intraparticle diffusion based on the concentration in solids (cm^2 s^{-1}). The straight line plots between log $[1 - (q_t/q_e)^2]$ and t (figure not shown) for different initial concentrations indicate the validity of Urano and Tachikawa equation developed for the intraparticle diffusion controlled mechanism. The D_i values were found to decrease from $8.54\pm0.40\times10^{-14}$ to $7.10\pm0.30\times10^{-14}$ cm^2 s^{-1} when the initial concentration increases from 100 to 250 mg L^{-1}. The values of R^2 obtained from these studies are greater than that of the external mass transfer diffusion process, so intraparticle mass transfer process was best suited. Moreover according to the literature [30] it is evident that the removal of U(VI) follows a intraparticle mass transfer diffusion process since the D_i values are in the order of 10^{-14} cm^2 s^{-1}.

3.3.3. Effect of pH

The adsorption behavior of the functionalized groups of adsorbent towards metal ion removal depends on the protonation and deprotonation properties of its acidic and basic groups, accordingly, the adsorption behavior is greatly affected by pH value. The availability of HA-Zr-PILC for U(VI) complexation was investigated at different pH values in the range of 2.0–7.0 (Fig. 11). This is
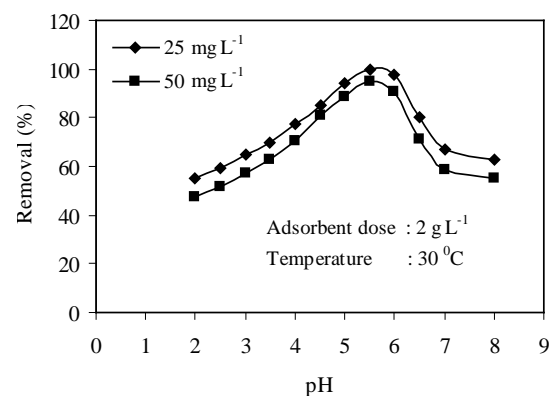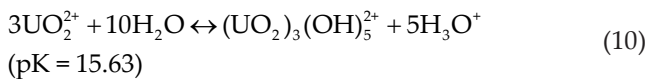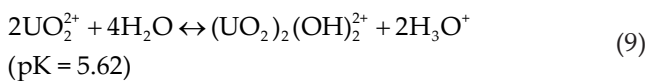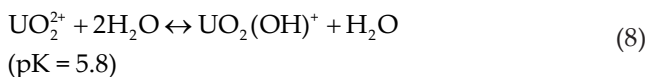

Fig. 11. Effect of pH for the adsorption of U(VI) ions onto HA-Zr-PILC.

because at high pH values, precipitation occurs, which effects the accuracy of the sorption study. It is clear that adsorption of uranyl ion onto HA-Zr-PILC was maximum at pH 6.0. Uranium loading by adsorbent increased with increasing pH from 3.0 to 6.0, reaches a maximum value at pH 6.0, and then decreases with increasing pH. The decrease of U(VI) onto HA-Zr-PILC at pH > 6.0 may be explained in terms of pH_{zpc} of the adsorbent and U(VI) species in solution. As all the batch experiments have been conducted in aerobic conditions, the presence of dissolved carbonates can also influence the speciation of uranyl ions. The formation of soluble ionic form of uranyl carbonate ions, $UO_2(CO_3)_2^{2-}$ and/or $UO_2(CO_3)_3^{4-}$ [31] may lead to decrease in adsorption of uranium onto negatively charged surface of the HA-Zr-PILC. As the pH decrease, the surface of the adsorbent exhibits increasing positive characteristics. Since the species to be adsorbed are also positive, the adsorption is not favored. Besides this H+ ions present at higher concentrations in the reaction mixture competes with positive ions for adsorption sites resulting in the reduced uptake of uranium. On the contrary, as the pH increases, the adsorbent surface becomes more and more negatively charged due to the ionization of humic acid ($HA + H_2O \rightarrow H_3O^+ + A^-$) which results in the concentration of negatively charged ion A⁻ and hence the adsorption of positively charged species is more favorable.

Various hydroxo complexes of uranium may form when the pH increases from acidic value to the neutral value. The relative protonation of these species is determined by the pH and total uranium concentration. Repartition of the hydroxo complexes is determined by the following equilibria [32].

$$UO_2^{2+} + 2H_2O \leftrightarrow UO_2(OH)^+ + H_2O \quad (8)$$
(pK = 5.8)

$$2UO_2^{2+} + 4H_2O \leftrightarrow (UO_2)_2(OH)_2^{2+} + 2H_3O^+ \quad (9)$$
(pK = 5.62)

$$3UO_2^{2+} + 10H_2O \leftrightarrow (UO_2)_3(OH)_5^{2+} + 5H_3O^+ \quad (10)$$
(pK = 15.63)

At pH 6.0, where the U(VI) removal from the solution take its maximum value, the dominant species of U(VI) ions exist in solution as UO_2OH^+. The fall in pH during the adsorption process, which clearly indicates the rise in the proportion of cation sorbed, is in keeping with the occurrences of cation exchange reaction of the kind shown below.

$$\text{HA-Zr-PILC-COOH} + UO_2OH^+ \rightarrow$$
$$\text{HA-Zr-PILC-COO-UO}_2OH + H^+ \quad (11)$$
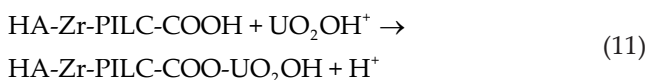
3.3.4. Adsorption isotherm

3.3.4.1. Equilibrium modeling

Several adsorption isotherm models including Langmuir, Freundlich and Redlich–Peterson [33] isotherms, were tested for simulation of experimental equilibrium data.

The Langmuir adsorption isotherm:

$$q_e = Q^0 bC_e \big/ 1 + bC_e \quad (12)$$

The Freundlich adsorption isotherm:

$$q_e = K_F C_e^{1/n} \quad (13)$$

The Redlich–Peterson isotherm

$$q_e = \frac{K_k C_e}{a_R C_e} b + 1 \quad (14)$$

where q_e and C_e are the equilibrium concentrations of the uranium on adsorption. Q^o and b are Langmuir constants and K_F and $1/n$ are the Freundlich constants and K_R, b and a_R are the R–P constants related to adsorption capacity and intensity of adsorption, respectively. The experimental and model fit of q_e and C_e for the adsorption of U(VI) are shown in Fig. 12. The values of isotherm constants are listed in Table 2. The values of R^2 and χ^2 (Table 2) obtained for the adsorption of uranium on the HA-Zr-PILC follow Langmuir adsorption isotherm. The fact that the Langmuir isotherm fits the experimental data very well may be due to homogenous distribution of active sites on the HA-Zr-PILC surface, since the Langmuir equation assumes that the surface is homogeneous. The adsorption capacity Q^o found in this study for U(VI) was higher than the ones reported in the literature. The values of Q^o for the adsorption of U(VI) were reported to be 58.43, 18.72, 28.49, 28.30 and 15.10 mg g⁻¹ onto mesoporous silica [34], diarylazobisphenol modified carbon [35], modified
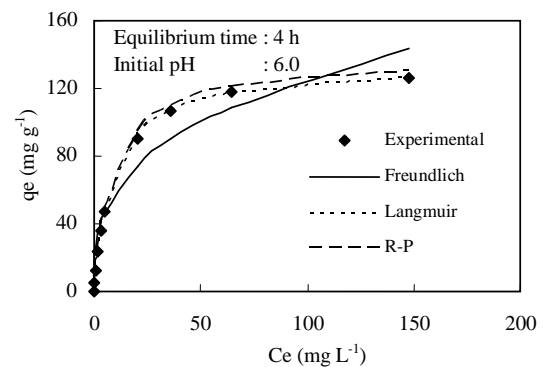

Fig. 12. Comparison of the experimental and model fits of the Langmuir, Freundlich and R–P isotherms (lines) for the adsorption of U(VI) onto HA-Zr-PILC.

Table 2
Isotherm constants for the adsorption of U(VI) onto HA-Zr-PILC

Langmuir	
Q^0 (mg g^{-1})	134.654.07±4.72
b (L mg^{-1})	0.020±0.001
R^2	0.99
χ^2	1.11
Freundlich	
K_F	14.06±0.53
$1/n$	0.331±0.013
R^2	0.94
χ^2	3.73
Redlich–Peterson	
K_R	33.00±0.36
b	0.60±0.02
a_R	1.43±0.03
R^2	0.95
χ^2	6.75

Table 3
Four cycles of uranyl adsorption–desorption with 0.1 M HCl as the desorbing agent

Cycle	Adsorption (mg g^{-1})	Desorption (%)	(%)
1	12.30±1.51	99.2±1.2	94.2±2.4
2	12.10±1.10	97.3±1.5	92.0±3.1
3	11.80±1.51	96.2±1.6	91.1±1.2
4	11.50±0.81	94.5±3.2	89.0±2.3
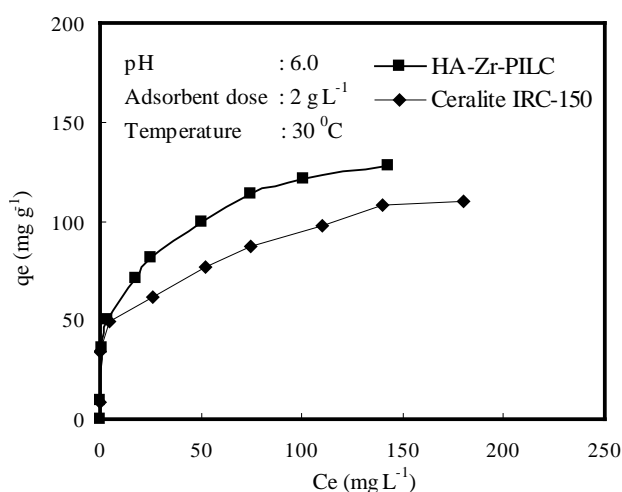
Fig. 13. Comparison of the adsorption of U(VI) onto HA-Zr-PILC and Ceralite IRC-150 at 30°C.

carbon [36], activated carbon [37] and manganese oxide-coated zeolite [38] respectively.

3.3.5. Desorption and regeneration studies

Desorption is an important process in adsorption studies because it enhance the economical value of adsorption process. Desorption study will help to regenerate the spent adsorbent so that it can again be reused to adsorb metal. Desorption efficiency of the spent adsorbent was checked with HCl solution having different concentrations (0.001–0.1 M). The results demonstrated that the adsorbed U(VI) could be desorbed from the spent adsorbent using 0.1 M HCl and hence for obtaining the versatility of the HA-Zr-PILC, the adsorption–desorption cycle was repeated four times with same adsorbent using 0.1 M HCl. From Table 3 it is clear that the adsorbed quantity of 99.2±1.2% of uranium ion, 94.2±2.4% was desorbed by 0.1N HCl. After four cycles adsorption capacity of HA-Zr-PILC was decreased from 99.2±1.2 to 94.5±3.2% and the recovery of HA-Zr-PILC in 0.1N HCl decrease from 94.2±2.4 to 89.0±2.3%. Therefore HCl can regenerate the adsorbent effectively.

3.3.6. Comparison with commercial adsorbent

For comparison, isotherm test for the adsorption of U(VI) ion onto a commercial ion exchanger Ceralite IRC–50 with carboxylic acid functionality is also performed and the results are shown in Fig. 13. The Langmuir isotherm parameters were obtained using non-linear regression analysis. The higher value of R^2 (0.99) obtained for Freundlich model indicates that this model could define

the experimental results in the Ceralite IRC-50-U(VI) system. The calculated values of Q^o and b were found to be 95.81±3.10 mg g^{-1} and 0.061±0.003 L mg^{-1}, respectively which were lower than those calculated for HA-Zr-PILC.

3.3.7. Test with simulated nuclear industry wastewater

The simulated U(VI) nuclear industry wastewater sample was treated with HA-Zr-PILC to demonstrate its adsorption potential and utility in removing U(VI) ion from wastewater in the presence of other ions. Wastewater sample was prepared according to the composition reported in the literature [39]. The sample contained apart from U(VI) (10 mg L^{-1}) other metal ions based on cations such as Ca^{2+} (10 mg L^{-1}), Mg^{2+} (10 mg L^{-1}) as well as anions such as Cl$^-$ (20 mg L^{-1}), SO$_4^{2-}$ (80 mg L^{-1}), NO$_3^-$ (40 mg L^{-1}), PO$_4^{3-}$ (20 mg L^{-1}), oxalate (60 mg L^{-1}) and detergents (20 mg L^{-1}). The effect of adsorbent dose on U(VI) removal from wastewater was investigated (Fig. 14). It can be seen that the percentage of U(VI) adsorption increases with increasing HA-Zr-PILC dosage and almost complete removal (100%) of U(VI) from a wastewater sample containing 10 mg L^{-1} was achieved with 2 g HA-Zr-PILC in
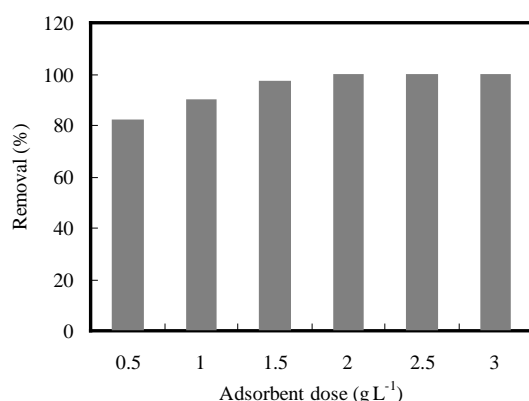
Fig. 14. U(VI) ion removal from simulated nuclear industry wastewater by HA-Zr-PILC.

one liter, which is in agreement with that obtained from the batch experiments as mentioned above.

4. Conclusions

In the present study, a novel adsorbent, humic acid immobilized Zr-PILC (HA-Zr-PILC) was prepared and its efficiency in removing U(VI) was tested by batch adsorption technique. The pH 6.0 was found to be optimum for the adsorption of U(VI) on pillared clay Upon various models applied the pseudo-second-order, intraparticle diffusion kinetic models and Langmuir isotherm model gave good correlation with the experimental data. Attempts for quantitative removal of U(VI) from nuclear industry effluent wastewater using HA-Zr-PILC were made and satisfactory results were obtained. Repeated adsorption–desorption study showed that HA-Zr-PILC can be effectively used as an adsorbent for the removal and recovery of U(VI) from aqueous solutions.

Acknowledgments

References

[1] US EPA, EPA Integrated Risk Information System (IRIS). Electronic Database. US Environmental Protection Agency, Washington, DC,1996.
[2] G.A. Aycik and R. Gurellier, J. Radioanal. Nucl. Chem., 273 (2007) 713–718.
[3] A.A. Atea, Hydrometal., 80 (2005) 13–22.
[4] B.L. Rivas, H.A. Maturama, X. Ocampo and I.M. Peric, J. Appl. Polym. Sci., 58 (1995) 2201–2205.
[5] U. Ulosoy, S. Simsek and O. Ceyhem, Adsorption, 9 (2003) 165–175.
[6] M.F. El-Shahet, E.A. Moawed and A.B. Farag, Talanta, 71 (2007) 236–241.
[7] T.S. Anirudhan, L. Divya and P.S. Suchithra, J. Environ. Manag., 90 (2008) 549–560.
[8] C. Hennig, T. Reich, R. Daha and A.M. Scheidegger, Radiochim. Acta, 90 (2002) 653–657.
[9] H. Ketsumata, S. Kaneco, K. Inopmota, K. Itoh, K. Fumasaka, K. Masuyama, T. Suzuki and K. Ohte, J. Environ. Manag., 69 (2003) 187–191.
[10] W. Mathews, F.T. Madsen and G. Kahr, Clays Clay Miner., 47 (1999) 617–629.
[11] C. Cooper, J.Q. Jeang and S. Quki, J. Chem. Technol. Biotechnol., 77 (2002) 548–551.
[12] D. Manohar, B.F. Noeline and T.S. Anirudhan, Appl. Clay Sci., 31 (2006) 194–206.
[13] S. Amin and G.G. Jayson, Water Res., 30 (1996) 299–306.
[14] V.P. Vinod, S. Varghese and T.S. Anirudhan, Indian J. Chem. Technol., 10 (2003) 201–210.
[15] C.D. Bringle, I.G. Shibi, V.P. Vinod and T.S. Anirudhan, J. Sci. Ind. Res., 46 (2005) 782–788.
[16] H. Bennet and R.A. Reed, Chemical Methods of Silicate Analysis. Academic Press, New York, 1971.
[17] A. Dyer, T. Galiardo and C.W. Roberts, Preparation and properties of clays pillared with zirconium and their use in HPLC separations. In Zeolites: Facts, Figures, Future, P.A. Jacob and R.A. Vansanten, eds., Elsevier, Amsterdam, 1989.
[18] S. Viladker, R. Agarwal and B. Kamaludhin, Bull. Chem. Soc. Jpn., 69 (1996) 95–100.
[19] J.A. Schwarz, C.T. Driscoll and A.K. Bhanot, J. Colloid Interface Sci., 97 (1984) 55–61.
[20] D.M. Manohar, B.F. Noeline and T.S. Anirudhan, Ind. Eng. Chem. Res., 44 (2005) 6676–6684.
[21] E.B. Sandell, Colorimetric Determination of Traces of Metals, Interscience Publishers, New York, 1944.
[22] D.S. Orlor, Soil Chemistry. Oxford & IBH. Publishing, New Delhi, 1992.
[23] V.P. Vinod and T.S. Anirudhan, Wat. Air Soil Pollut., 150 (2003) 193–217.
[24] G. Rytwo, D. Tropp and C. Serban, Appl. Clay. Sci., 20 (2002) 273–282.
[25] C. Nathalie, G. Richard and D. Eric, Water Res., 37 (2003) 3079–3086.
[26] T.S. Anirudhan and P.G. Radhakrishnan, J. Colloid Interface Sci., 316 (2007) 268–276.
[27] K. Anoop Krishnan and T.S. Anirudhan, J. Hazard Mater., B92 (2002) 161–183.
[28] G. McKay, M.S. Otterburn and A.G. Sweeny, Water Res., 15 (1981) 327–331.
[29] K. Urano and H. Tachikawa, Ind. Eng. Chem. Res., 30 (1991) 1897–1899.
[30] V.P. Vinod and T.S. Anirudhan, J. Chem. Technol. Biotechnol., 77 (2001) 92–101.
[31] N. Zhiwei, F. Qiahui, W. Wenhuc, X. Junzheng, C. Lei and W. Wangsuo, Appl. Radiation Isotopes, 9 (2009) 1582–1590.
[32] M.Z.C. Hu, J.M. Norman, N.B. Faison and M. Reeves, Biotechnol. Bioeng., 51(1996) 237–247.
[33] W.T. Tsai, H.C. Hsu, T.Y. Su, K.Y. Lin and C. M. Lin, J. Colloid Interface Sci., 299 (2006) 513–519.
[34] K. Stomberg, K.A. Venkatesan and P.R. Vasudeva Rao, Colloids Surf. A: Physiochem. Eng. Aspects, 221 (2003) 149–162.
[35] A.M. Starvin and T.P. Rao, Talanta, 2 (2004) 225–232.
[36] C. Kutahyali and E. Meral, Sep. Purif. Technol., 40 (2004) 109–114.
[37] A. Mallah, S. Chagrouche and M. Barkat, J.Colloid Interface Sci., 296 (2006) 434–441.
[38] R. Han, W .Zou, Y. Wang and L. Zhu, J. Environ. Radioactivity, 93 (2007) 127–143.
[39] M. Jansson-Charrier, E. Guibel, J. Roussy, R. Surgons and P. Le Cloirec, Water Sci. Technol., 34 (1996) 169–177.